More Effective Robotic UV Disinfection of Objects Through Human Guidance

Alan G. Sanchez
Oregon State University
Corvallis, Oregon, USA
sanchala@oregonstate.edu

Nash Bernhart
Oregon State University
Corvallis, Oregon, USA
bernharn@oregonstate.edu

William D. Smart
Oregon State University
Corvallis, Oregon, USA
bill.smart@oregonstate.edu

ABSTRACT

Ultraviolet-C (UV-C) robot irradiation is a promising approach for disinfecting surfaces contaminated by pathogens in healthcare settings. However, limitations exist with current UV disinfection robots, including coverage for complex surface geometries. This research presents a system for human-guided robotic UV disinfection that uses empirical sensor measurements rather than relying on high-accurate models for UV map coverage. Human guidance is integrated into the methodology to enhance disinfection, aiding in addressing complex shaped objects and topologies. Further, a validation test confirmed that our estimation approach reliably underestimates the UV exposure, which is beneficial for ensuring thorough disinfection. Initial pilot studies demonstrated that while autonomous disinfection was effective for simple objects like tabletops, human-guided disinfection, especially with feedback, improved coverage and speed for complex shapes like mugs. Combining human intuition with autonomy shows promise for enhancing robotic disinfection effectiveness.

CCS CONCEPTS

• **Computing methodologies → Model verification and validation**.

KEYWORDS

UV disinfection, UVC, Semi-autonomous robots, Sterilization

ACM Reference Format:
Alan G. Sanchez, Nash Bernhart, and William D. Smart. 2024. More Effective Robotic UV Disinfection of Objects Through Human Guidance. In *Companion of the 2024 ACM/IEEE International Conference on Human-Robot Interaction (HRI '24 Companion), March 11–14, 2024, Boulder, CO, USA.* ACM, New York, NY, USA, 5 pages. https://doi.org/10.1145/3610978.3640683

1 INTRODUCTION

In the past decade, healthcare settings have faced challenges posed by highly contagious pathogens, particularly impacting healthcare personnel working in contaminated spaces [16]. Surface contamination is a known factor in nosocomial transmissions [8–10], making effective disinfection crucial. Recent efforts have led to the development of UV-C robots for combating infectious diseases, particularly those transmitted through surface contact [1, 6, 11, 12, 14]. However, existing designs encounter limitations in disinfecting surfaces with small-scale occlusions [7], such as tools on a table.

Our prior work leveraged a robotic arm holding a UV light source to cover small-scale surfaces [13]. We developed a framework that accurately modeled a non-uniform light distribution while regulating the velocity control of the manipulator to ensure sufficient virus inactivation. In our current research, we extend the previous study by addressing challenges in environmental modeling by adopting a direct empirical measurement of UV light to create coverage maps. To ensure the validity of our measurement technique, we compared our data against readings from accurate sensor modules in a test article.

We have also incorporated human input as a component of our disinfection methodology. With the variability of shape, size, and accessibility of objects, human input is employed to determine optimal disinfection paths. Human input can allow us to include semantic knowledge of object features, such as handles and occlusions, potentially enhancing our system to create paths to help cover commonly missed sections.

2 RELATED WORK

There has been growing research interest in robots involved with virus inactivation to keep up with sanitation standards. Mehta *et al.* [5] provides an overview of the effectiveness and current state of UVGI robots. They discuss the needed improvements in dosage modeling, human safety during deployment, and semantic segmentation to identify high-risk surfaces for quicker disinfection.

Marquess *et al.* [4] introduces dosing constraints that result in lower disinfection time while ensuring adequate UV dose exposure to a surface. Their approximate algorithm selects feasible vantage configurations, which then create path networks and calculate irradiance matrices across the surfaces. Their algorithm then determines optimal dwell times and executes the tool path. The authors defined the optimization problem as computationally complex. Thus, they propose a two-stage approach that combines linear programming and the traveling salesman problem techniques for efficient coverage planning. Further, the method was tested in simulation for various UVGI robot designs, demonstrating its versatility. However, the algorithm has yet to be tested on an actively exploring system that might not account for unpredictable environmental factors or robot hardware limitations.

A challenge in modeling dose accumulation is effectively measuring a robot's disinfection performance. Kurniawan *et al.* [3] addresses this hurdle by simulating the coverage using an octree as a voxel-based representation of the environment. Their UVGI robot has a noiseless 3D LIDAR that projects discrete light rays into

HRI '24 Companion, March 11–14, 2024, Boulder, CO, USA

ACM ISBN 979-8-4007-0323-2/24/03
https://doi.org/10.1145/3610978.3640683

the simulated world. Then, each cube-shaped node in the octree stores the radiation dose value it receives from the light ray. Comparing their data with ground truth reference octree, their findings highlight the potential applications of their system for UVGI performance evaluation. Similar to the work conducted by Marquess, the study is confined to a simulated environment, and it considers a noiseless 3D LIDAR that can neglect inconsistencies found in actual sensor data. Although physics simulators can quickly provide insights into a design, it is important to note that they encounter real-world modeling mismatches that can negatively affect the performance of a system.

Our work draws parallels with Kurniawan's but extends this approach by measuring disinfection performance on hardware. We also represent the world as an octree, but rather than using a 3D LIDAR, we employ a color and depth perception camera to empirically measure the UV light distance and compute the dose captured in each node.

3 IMPLEMENTATION

Our system allows a human operator to demonstrate a trajectory for a UV flashlight, designed to disinfect an object or area on a tabletop. The robot can then replicate this trajectory to disinfect the object. We show that, when the human has access to a 3D visualization of the current status of the disinfection, they can disinfect more effectively than an autonomous system, often completing the task faster. We explicitly want to avoid building high-fidelity models of the objects we are disinfecting, to reduce our reliance on high-fidelity sensors and actuators.

3.1 System Hardware

For our robot, we utilized the Fetch mobile manipulator platform [15]. The robot is equipped with a holonomic base, a 7 degrees-of-freedom arm, a parallel-jaw gripper, and a movable head with an integrated PrimeSense camera. The PrimeSense camera comprises an RGB sensor and an infrared projector and sensor. These elements will enable the head camera to record the depth and color information needed in our design layout when representing the world as an oct-tree. The parallel-jaw gripper also holds the light source, a 10-watt 365 *nm* UV flashlight.

A RealSense D435 camera [2] was installed on the robot's end effector. Like the head camera, the RealSense can record the depth and color information from its images. The objective of the RealSense camera is to determine which nodes in the octree are experiencing UV exposure.

3.2 Octree Representation

Using the head camera, the robot captures a time-stamped point-cloud message type and builds a collection of 3D coordinate points with color information, of the contaminated space. When the robot is directed to execute a tool path for disinfection, the OctoMap package processes the most up-to-date point cloud message and builds an octree representation of the environment, as shown in Figure 1. For the purposes of evaluation in this paper, we further segment the area of tabletop and objects, so that we can measure disinfection rate more accurately. This segmentation step is not necessary to deploy the system.

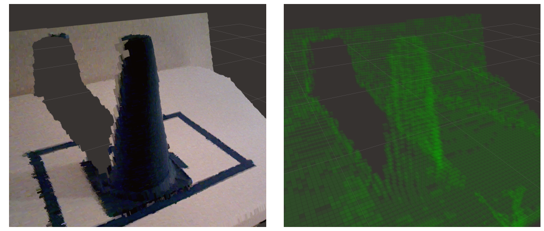

(a) Point cloud of cone. **(b) Built octree of the cone.**

Figure 1: Octree representation from head camera data.

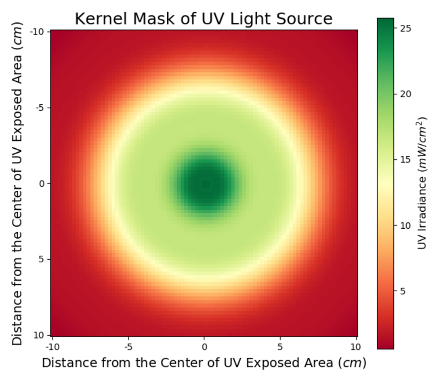

Figure 2: Model of the UV Flashlight.

To visualize the accumulated dosage, using the ROS RViz tool, cube markers are generated using the stored data. Their colors shift from red to orange, then yellow, and finally green, reflecting an order of increasing UV dose. Once a cube is highlighted green, it indicates that the node has acquired or exceeded the desired threshold. The cubes are published in real-time to provide feedback on the disinfection progress.

3.3 Image Processing

We use computer vision techniques to identify the illuminated spots from the RealSense's captured images. Our current implementation; however, performs in a slightly dimmed room and focuses on known colored objects. These environmental conditions allowed us to test and observe our disinfection method approach, and further development of our system, such as a UV-sensitive camera, can enable it to function in various lighting conditions.

Our process identifies which node is occupied by a point in the depth image. Using the node's coordinates, the system computes the relative angle from the UV light source's central line and the Euclidean distance between the node and UV light. The robot can then infer the dosage using the inverse square law, exposure time, and referencing our UV model, see Figure 2, where irradiance intensity attenuates the further a point is away from the flashlight's central line. The node's spatial and dose information is then stored. This process is continuous throughout the path, and if points in

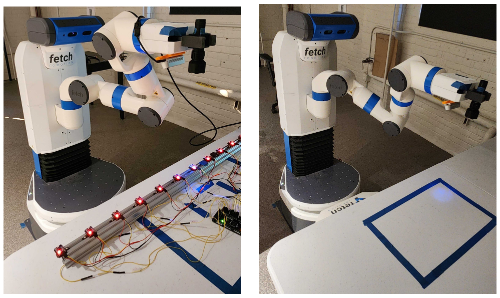

(a) Set up for Sensor Array. **(b) Set up for table disinfection.**

Figure 3: Apparatus set up for validation tests.

a node are repeated, the dose value is incremented, and the new cumulative dose is saved.

3.4 Programming by Demonstration Interface

Our interface was developed within the ROS framework[17] and is designed to record human-guided arm trajectories. The system primarily functions by subscribing to the joint states of the robot's arm, capturing any change in its position. Before a user guides the arm, the arm's control mechanisms are set to a relaxed state, allowing for external manipulation. A user can move and position with the arm with little resistance. After the user has finished guiding the arm, the joint states and other movement details are saved to a JointTrajectory message type. Our playback node offers the ability to reproduce the guided trajectory and execute the stored movements in their original duration or adjust to different speeds. The interface provides a method for capturing and reproducing robotic arm movements based on user input without the need for manual programming.

4 VALIDATION EXPERIMENT

To ensure that we are able to get accurate estimates of irradiation, we performed a validation experiment. We generated a 1D trajectory for the table and as well for a sensor array. The Sensor array is equipped with UV sensor modules and is approximately one meter long. Each sensor was calibrated to work with our flashlight's UV band range. The sensor array was positioned on a flat tabletop in front of the robot, as shown in Figure 3a.

To validate the system, we performed ten repetitions of the trajectory for each setup, see figure 5, recording both the directly measured irradiance from the sensor array and our computational estimate measured by the end effector camera. The data is shown in Figure 4. The first thing to note is that the computational estimate follows the actual measured value, but consistently under-estimates it. While a more accurate estimate is often desirable, in the case of UV disinfection, we strongly prefer to have consistent under-estimation. This means that, if we use the computational estimate, we will tend to over-irradiate the objects being disinfected (which is fine), rather than under-irradiating them (which will lead to incomplete inactivation of the virus, which is bad).

The under-estimation is, in part, caused by measurement noise in the distance sensor. This leads to some irradiation being allocated

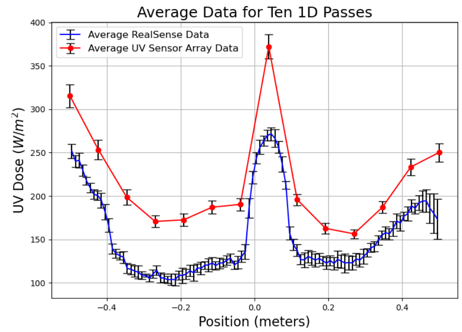

Figure 4: Average measured UV dose (red) and average computational estimate of dose (blue).

to a cell that is actually inside the surface of the sensor. This, in turn, leads to less accumulated irradiation in the surface cell. Given our commitment to using approximate octree models and commercially-available sensors, this is unavoidable. It is, however, tolerable, since it will only lead to under-estimation and never over-estimation.

5 PILOT STUDY

5.1 Study Layout

To provide some initial evaluation for our approach, we performed a pilot study to show how human guidance affects disinfection rates and coverage. For this experiment, we focused on three test objects: a cone, a mug, and a delineated part of the flat surface of a table. The table has simple geometry and topology and provides a baseline. The cone offers a simple convex surface with no affordances; a slightly more complex geometry, but still simple topology. Finally, the mug has both a more complex geometry and topology. It also has affordances, not apparent from either the geometry or topology, related to its *use*. The handle and the rim are more important disinfection targets, since these areas are the ones where humans will most interact with the object. Performing a more complete disinfection here may be important, and is something best done with human guidance. We note, however, that we do not evaluate these affordance-based disinfection targets, leaving this for future work.

The experiment has three conditions: autonomous, no-feedback, and with-feedback. In the autonomous condition, the robot follows a pre-specified trajectory specific to the object being disinfected. In the no-feedback condition, a human guides the flashlight manually, directly moving the robot arm. In the with-feedback condition, a human also guides the flashlight manually, but also is shown a real-time visualization of the current disinfection status, as described above. Figure 5 shows the visual representation of the tabletop after a successful disinfection.

5.2 Systematic Errors

Note that, because of measurement errors in the distance sensor, disinfection is sometimes attributed to cells that are actually below the surface of the table. These are the red-colored cells in the view from below the tabletop oct-tree model, see 5b. This leads to a slight

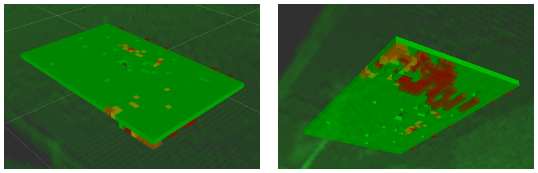

(a) Top View (b) Bottom View

Figure 5: Top and bottom views of the octree representation of the table.

Object	Auton.	Feedback?	S1	S2	S3
Tabletop	98.57%	No	50.25%	17.87%	34.22%
		Yes	97.34%	98.57%	98.27%
Cone	94.44%	No	75.98%	49.20%	86.41%
		Yes	87.38%	95.51%	83.03%
Mug	79.61%	No	49.69%	65.00%	50.50%
		Yes	89.84%	85.00%	88.45%

Table 1: Disinfection rates for the three objects for the autonomous system and the three subjects, in both the no-feedback and with-feedback conditions.

Object	Auton.	Feedback?	S1	S2	S3
Tabletop	17.82	No	111.77	46.27	49.24
		Yes	70.82	68.02	86.14
Cone	80.30	No	25.63	23.02	32.45
		Yes	43.58	65.72	42.65
Mug	42.43	No	18.45	20.71	15.98
		Yes	35.73	27.82	37.78

Table 2: Disinfection times, in seconds, for the three objects for the autonomous system and the three subjects, in both the no-feedback and with-feedback conditions.

Object	Auton.	Feedback?	S1	S2	S3
Tabletop	2.00	No	1.11	0.56	0.89
		Yes	3.24	2.33	2.91
Cone	6.35	No	1.94	1.31	1.41
		Yes	3.63	5.02	2.94
Mug	4.78	No	1.14	2.85	1.05
		Yes	3.23	3.65	6.46

Table 3: Average per-cell dose, as a proportion of the nominal disinfecting dose, for the autonomous system, without visual feedback, and with visual feedback.

under-estimate of the irradiation (as explained above), but also results in these cells being shown as being under-disinfected when, in reality, they are not (since they are inside the table). To address this, our analysis removes these cells from consideration in the analysis that follows. More specifically, we heuristically remove cells that have a computed irradiation value less than 50% of the smallest of their neighbors. In our tests, this proved to reliably get rid of these spurious cells. Ideally, we would form a model of the object, and analytically determine which cells were inside; however, in this paper we make the explicit commitment not to model the object in this way, leaving a heuristic pruning of cells the only viable option. A separate analysis was performed on the un-pruned estimates and, in all cases, the trend followed that reported here, with improvements in disinfection showing in the same conditions, with approximately the same magnitude. However, we feel that the pruned results better represent the actual level of surface disinfection occurring.

5.3 Preliminary Results

Table 1 summarizes the disinfection rates from the experiments. The autonomous disinfection is highly effective for the tabletop, resulting in 98.57% of the area receiving a sufficient dose to inactivate our notional virus. The autonomous system is also highly effective in disinfecting the cone, with 94.44% disinfected cells. It can also be observed that humans perform better with visual feedback, and in the instance of the mug, feedback did better than the autonomous path.

Table 2 displays the disinfection times of the three different conditions. Interestingly, providing feedback consistently increases the time taken by the subjects. This can be explained, in part, by having to look at the visualization and correlate it with the object, but also by the time taken to perform the higher level of disinfection noted in the figures above. For the tabletop, the autonomous system was markedly faster than all of the subjects, because of the simplicity of the trajectory it followed. However, for all other objects, humans were faster than that autonomous system, presumably because of their intuitions about how to illuminate the more complex objects.

Finally, Table 3 shows the average per-cell dose delivered in the various conditions. Unsurprisingly, humans deliver more average doses in the with-feedback condition. However, they generally deliver less average dose than the autonomous system for both the cone and the mug, presumably because the guided trajectories are more efficient and less redundant than those used by the autonomous system.

6 DISCUSSION

This work demonstrates the potential benefits of incorporating human guidance and feedback for robotic UV disinfection without relying on high-accurate models. The disinfection experiments compared three conditions: autonomous disinfection, human-guided with no feedback, and human-guided with visual feedback. On objects with simple geometry, like the tabletop, the autonomous system performed disinfection quickly and effectively. However, the cone and mug results show that human intuition can improve coverage and sometimes speed for complex topologies, especially when visual feedback is provided.

Although these findings are insightful, it is important to highlight this research's limitations. We consider this work a preliminary study, but also acknowledge that this creates the beginning works for broader, more detailed investigations.

ACKNOWLEDGMENTS

The authors would like to thank Zachary I. Lee and Kyle DuFrene for their involvement in the experiments described in this paper.

REFERENCES

[1] Moez Guettari, Ines Gharbi, and Samir Hamza. 2021. UVC disinfection robot. *Environmental Science and Pollution Research* 28 (2021), 40394–40399.

[2] Intel Corporation. 2023. The Intel RealSense D435. https://www.intelrealsense.com/depth-camera-d435/.

[3] Irfan Tito Kurniawan and Widyawardana Adiprawita. 2021. A method of ultraviolet-C surface irradiation simulation and evaluation. In *2021 International Symposium on Electronics and Smart Devices (ISESD)*. IEEE, 1–5.

[4] Joao Marcos Correia Marques, Ramya Ramalingam, Zherong Pan, and Kris Hauser. 2021. Optimized coverage planning for UV surface disinfection. In *2021 IEEE International Conference on Robotics and Automation (ICRA)*. IEEE, 9731–9737.

[5] Ishaan Mehta, Hao-Ya Hsueh, Sharareh Taghipour, Wenbin Li, and Sajad Saeedi. 2022. UV disinfection robots: a review. *Robotics and Autonomous Systems* (2022), 104332.

[6] Nikita Mikhailovskiy, Alexander Sedunin, Stepan Perminov, Ivan Kalinov, and Dzmitry Tsetserukou. 2021. Ultrabot: Autonomous mobile robot for indoor uv-c disinfection with non-trivial shape of disinfection zone. In *2021 26th IEEE International Conference on Emerging Technologies and Factory Automation (ETFA)*. IEEE, 1–7.

[7] Devin Mills, Delbert A Harnish, Caryn Lawrence, Megan Sandoval-Powers, and Brian K Heimbuch. 2018. Ultraviolet germicidal irradiation of influenza-contaminated N95 filtering facepiece respirators. *American journal of infection control* 46, 7 (2018), e49–e55.

[8] JA Otter, C Donskey, S Yezli, S Douthwaite, SDea Goldenberg, and DJ Weber. 2016. Transmission of SARS and MERS coronaviruses and influenza virus in healthcare settings: the possible role of dry surface contamination. *Journal of Hospital Infection* 92, 3 (2016), 235–250.

[9] Jonathan A Otter, Saber Yezli, and Gary L French. 2011. The role played by contaminated surfaces in the transmission of nosocomial pathogens. *Infection Control & Hospital Epidemiology* 32, 7 (2011), 687–699.

[10] Jonathan A Otter, Saber Yezli, James AG Salkeld, and Gary L French. 2013. Evidence that contaminated surfaces contribute to the transmission of hospital pathogens and an overview of strategies to address contaminated surfaces in hospital settings. *American journal of infection control* 41, 5 (2013), S6–S11.

[11] Alyssa Pierson, John W Romanishin, Hunter Hansen, Leonardo Zamora Yañez, and Daniela Rus. 2021. Designing and deploying a mobile UVC disinfection robot. In *2021 IEEE/RSJ International Conference on Intelligent Robots and Systems (IROS)*. IEEE, 6700–6707.

[12] Thomas Rubaek, Merima Cikotic, and Simon Falden. 2016. Evaluation of the UV-disinfection robot. *Blue Ocean Robotics* (2016).

[13] Alan G Sanchez and William D Smart. 2021. A Shared Autonomy Surface Disinfection System Using a Mobile Manipulator Robot. In *2021 IEEE International Symposium on Safety, Security, and Rescue Robotics (SSRR)*. IEEE, 176–183.

[14] Luca Tiseni, Domenico Chiaradi, Massimiliano Gabardi, Massimiliano Solazzi, Daniele Leonardis, and Antonio Frisoli. 2021. UV-C Mobile Robots With Optimized Path Planning. *Robotics & Automation Magazine* 28, 1 (2021), 59–70.

[15] Melonee Wise, Michael Ferguson, Derek King, Eric Diehr, and David Dymesich. 2016. Fetch and freight: Standard platforms for service robot applications. In *Workshop on autonomous mobile service robots*.

[16] World Health Organization. 2015. Ebola Situation Report. https://apps.who.int/ebola/current-situation/ebola-situation-report-4-november-2015

[17] ZebraDevs. 2023. fetch_ros: Fetch Robotics ROS Package. https://github.com/ZebraDevs/fetch_ros.